Initial growth mode of ultrathin Ag films on an Al(111) surface

S. H. Kim,[1] Jikeun Seo,[2] Y. Shin,[3]* W. Kim,[4] C. Y. Park,[1] S.-J. Oh,[4] J. M. Seo,[5] H. G. Min,[6] and J.-S. Kim[3]
[1]*Department of Physics, Sungkyunkwan University, Suwon Kyungkido, Korea*
[2]*Division of General Education, Chodang University, Muan 524-800, Korea*
[3]*Department of Physics, Sook-Myung Women's University, Seoul 140-742, Korea*
[4]*Department of Physics, Seoul National University, Seoul 151-742, Korea*
[5]*Department of Physics, Jeonbuk National University, Jeonju 561-756, Korea*
[6]*Department of Physics, Hongik University, Seoul 121-791, Korea*
(Received 3 April 2000; revised manuscript received 14 September 2000; published 7 February 2001)

The initial growth mode of ultrathin Ag films grown on an Al(111) surface was studied using Auger electron spectroscopy, low-energy electron diffraction (LEED) and x-ray photoelectron spectroscopy. Although Al and Ag have the same fcc bulk structure with nearly the same lattice parameters and a similar homoepitaxial growth mode, the initial growth mode of Ag on an Al(111) surface showed quite an unexpected behavior. As silver was deposited on an Al(111) surface at room temperature, the intensities of LEED spots diminished exponentially up to about 2 monolayer (ML), and the LEED pattern completely disappeared between 2 to 4 ML coverage. After 4 ML thick deposition, (1×1) LEED pattern started to reappear. To explain these experimental results, we propose a growth model of Ag film on the Al(111) surface that incorporates stacking faults induced by an interface alloy formation as observed in our spectroscopic work.

DOI: 10.1103/PhysRevB.63.085414 PACS number(s): 68.35.−p, 68.55.−a

I. INTRODUCTION

In recent years, thin-film growth has become one of the main processes for information technologies such as magnetic storage media and microelectronic devices. One of the goals in thin-film growth is to find growth parameters for the fabrication of smooth surfaces and abrupt interfaces. As a result, the initial growth mode and morphology of thin films have drawn vast attention from researchers on both experimental and theoretical sides.[1,2]

Most of the work on the ultrathin film growth reveals that the growth modes are very diverse depending on the physical characteristics of the adsorbate and substrate materials such as their surface free energies, lattice parameters and crystalline structures.[1,2] The strain induced by the lattice mismatch plays a significant role in the determination of the initial growth mode for some systems.[3] Aside from the above-mentioned factors, stacking faults in the growing film[4] or surface alloying, results in complicated growth behaviors.[5–7]

Bulk Ag and Al have fcc structures, and their lattice parameters are 2.889 and 2.863 Å, respectively. The lattice mismatch between Ag and Al is only ~0.9%. Therefore, a pseudomorphic Ag film on an Al(111) should be under negligible stress. Ag(111) and Al(111) do not reconstruct, and the interlayer relaxations between the top two layers are negligible.[8] In those respects, the two surfaces are similar. On the other hand, Al (1.16 J/m^2) has smaller surface free energy than Ag (1.25 J/m^2),[9] and Al segregates to the surface in a bulk alloy of Al and Ag ($\geqslant$3% Ag concentration). Since the heat of mixing between the two materials is negative (−0.61 eV),[10] they can easily form alloys over the whole range of composition in their bulk state.[11] Most of the experimental studies on the growth of thin films involving Al such as Al/Au(111),[12] Al/Pt(111),[13] Pd/Al(100),[14] Fe/Al(100),[15] Al/Ag(110), and Al/Ag(111) (Ref. 16) report the formation of surface alloys. From the above results, we may also expect that Ag deposited on an Al(111) surface would form an alloy near the interface region. In the former studies on the Ag/Al(111) system,[17–20] however, the role of the possible surface alloying to the growth mode of a Ag film on an Al(111) surface was not given full consideration. Instead, the Stransky-Krastanov growth mode[17] or 3d island growth (Volmer-Weber mode)[18] were suggested for the growth mode of the Ag films on an Al(111) without the consideration of the alloying.

In this paper, we report on the spectroscopic evidence of alloy formation during the initial growth of Ag films on an Al(111) surface at room temperature. We will demonstrate that the loss of long-range order (LRO) as suggested by the disappearance of low-energy electron diffraction (LEED) patterns, especially for Ag films in the range of 1–2 to 4 ML thickness is correlated with surface alloying. Finally, we propose a qualitative growth model of the Ag film on Al(111).

II. EXPERIMENT

All the experiments were performed in three separate ultrahigh vacuum chambers with base pressures of $4-7\times10^{-11}$ torr. The Al(111) sample was of a ''top-hat'' shape and was cut to expose a (111) surface within 0.5°. A clean Al(111) surface was prepared by repeated cycles of Ar^+ ion sputtering and annealing at 750 K until no contaminants were detected by Auger electron spectroscopy (AES) with a cylindrical mirror analyzer. The clean Al(111) surface showed a sharp threefold LEED pattern characteristic of an fcc(111) surface.

Ag was thermally evaporated from a 99.999% Ag wire that was wound around a tungsten filament (99.99%). The deposition rate was 1–1.5 ML/min. During the evaporation, the chamber pressure was kept below 4×10^{-10} torr. The Ag coverage was monitored with a quartz microbalance and the coverage or the microbalance was calibrated by the intensity

ratio of the AES peaks with transition energies of 66 eV for Al and 357 eV for Ag. Ag was deposited on an Al(111) not only at room temperature (RT), but at 50 K. The low-temperature deposition of Ag was intended to see the effect of the alloying of Ag with Al at the interface on the LRO. Because we expected that the alloying, if any, should be less activated at such a low temperature, 50 K than at room temperature. For that purpose, the Al(111) substrate was cooled down below 50 K by a closed-cycle He refrigerator, and the sample temperature was monitored by a chromel alumel thermocouple attached just next to the sample.

XPS experiments were carried out in a separate UHV chamber equipped with LEED optics, an x-ray source, and a concentric hemisphere analyzer (VG100 AX). The base pressure of this chamber was 7×10^{-11} torr and maintained below 2×10^{-10} torr during Ag evaporation. The Mg K-α line was used for the x-ray source, and the overall spectrometer resolution was estimated to be around 0.9 eV. Thickness calibration was done by a quartz microbalance and cross checked by the intensity ratio between Al $2p$ and Ag $3d$ core-level peaks.

Oxygen titrations were made to test the composition profiles of Ag films by dosing 6 Langmuir (L) of oxygen with the oxygen partial pressure maintained around 1×10^{-7} torr after Ag had been deposited. During oxygen dosing, the sample was kept at room temperature.

For Ag films thicker than 4 ML, where LEED patterns are recovered, LEED I/V (spot intensity versus electron energy) analysis was made to determine the atomic structure of the films. For the analysis, beam intensities were collected with an automated video LEED system.[21] I/V curve for four inequivalent beams between 40 to 400 eV were fitted using a Tensor LEED program.[22] Pendry's reliability (R) factor and Moruzzi's scattering phase shifts were used.[23] For the thermal vibration effects, Debye temperatures of 225 K for Ag and 430 K for Al were chosen.

III. RESULTS

The clean Al(111) surface showed sharp threefold LEED pattern with no other super-structures. As Ag was deposited on the Al(111) surface at room temperature, the sharp LEED pattern of the clean Al(111) surface degraded very rapidly (Fig. 1). For Ag coverages between 2 and 4 ML, no LEED pattern could be seen at all except a bright background for all incident electron energies up to 500 eV. The LEED pattern appeared again as the Ag thickness increased (Fig. 1). Below 2 ML of Ag coverage, beams retained threefold symmetry, but between 4 and 9 ML, the LEED pattern was nearly sixfold symmetric. This implies that the film was largely comprised of hcp stacking domains and/or 180° rotated twin fcc domains. As coverage increased beyond 9 ML, the contrast of spots becomes more and more threefold symmetric. No other superstructure was observed on Al(111) for all Ag coverages and temperatures between RT and 50 K. On the other hand, for the (001) surface of Al at RT, a (5×1) superstructure was observed before the LEED pattern disappeared as the thickness of Ag film increased.[24,25]

Figure 2(a) quantitatively illustrates the dramatic change

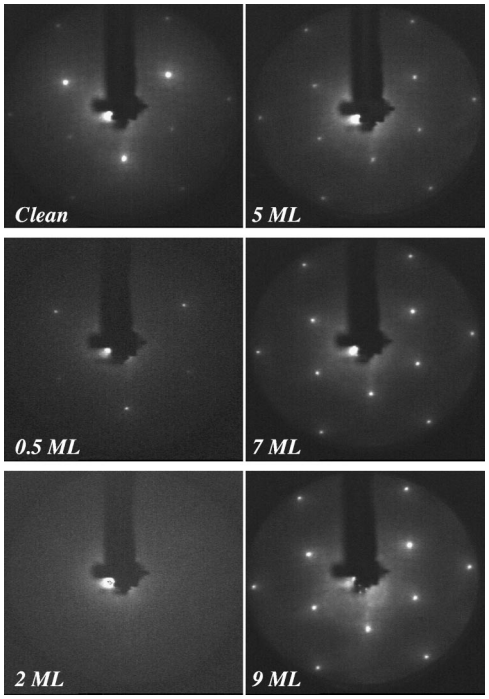

FIG. 1. LEED pattern for clean Al(111), and 0.5–9 ML Ag deposited on an Al(111) surface. Incident electron energy are 130 eV for all cases except 0.5 ML (80 eV).

of the (1, 0) LEED spot intensity as a function of the deposited Ag thickness. The intensity of the (1, 0) LEED spot diminished exponentially up to about 1 monolayer (ML) coverage, and then completely disappeared between 2 and 4 ML coverage. To examine the disorder normal to the plane separated from the lateral disorder, we examined the (0, 0) beam intensity near the out-of-phase condition with the sample 5° off from the normal direction. The (0, 0) beam is sensitive to the disorder in the direction normal to the surface because there is no lateral momentum transfer.[26] In Fig. 2(b), we also find an initial, rapid drop of the (0, 0) beam intensity, but not to the extinction of the LEED pattern. It suggests that there is substantial disorder of the structural and/or compositional origin along the surface normal direction. The disordered region is, however, not thick enough to completely dephase the scattered waves. On the other hand, the absence of (1, 0) spot intensity for all incidence energies up to 500 eV, which should include many in-phase conditions, indicates that there are severe lateral disorders in addition to the out-of-plane disorder for films below 4 ML.

Above 4 ML, the intensities of both (1, 0) and (0, 0) spots slowly recovered. As the silver coverage increased further, the overall spot intensities become similar to those from the clean Al(111) surface. The intensities and shapes of the LEED spots reflect the structural order of the surface. Thus, the intensity versus coverage data in Fig. 2 indicates that the surface loses its LRO in less than 2 ML of Ag due to both in- and out-of-plane disorder, and gradually recovers LRO after 4 ML of Ag are deposited.

LEED I/V analysis was performed for an 9 ML thick Ag/Al(111) system to determine the quality of the film after recovering LRO (Fig. 3). The best-fit model giving the low-

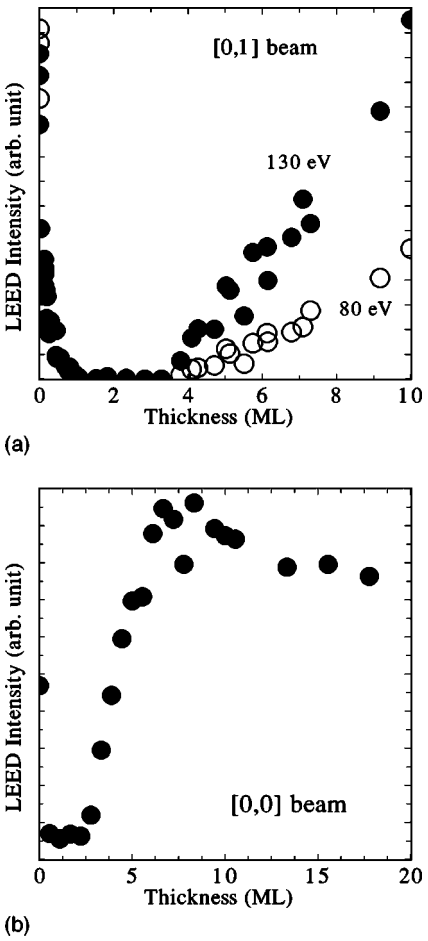

FIG. 2. LEED intensity versus Ag thickness. Averaged beam intensities are shown. (a) {0,1} beam at 130 eV (filled circle) and 80 eV (open circle) (b) {0,0} beam intensity at 52–54 eV.

est R factor is such that (1) the top layers within the reach of the probing electrons, about 3–4 ML, showed an expansion of their interlayer spacings (see Table I). Such an expansion of the layer spacings compensates the lateral contraction of the Ag film whose lattice parameter in their bulk phase is larger by 1% than that of Al. The interlayer spacing shows

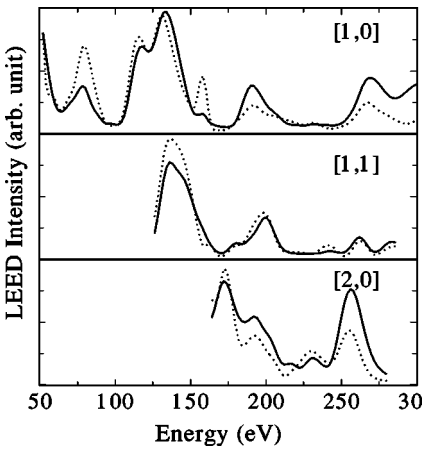

FIG. 3. Experimental (solid line) and theoretical (dotted line) LEED I/V curve for Ag (9 ML)/Al(111).

TABLE I. Best-fit structure of Ag (9 ML)/Al(111) from LEED I/V analysis. d_{ij} means the difference in the relative interlayer spacing between the ith layer and the jth layer from the interlayer spacing of the bulk terminated Al (111). The Pendry reliability factor was employed.

d_{ij}	Interlayer relaxation
d_{12}	+0.7%
d_{23}	+3.5%
d_{34}	+2.1%
d_{45}	+2.5%
R factor	0.2061

oscillatory behavior as usually found for bulk terminated surfaces. (2) The film is found to be composed of two, 180° rotated twin domains of fcc stacking with almost equal population in consistency with the observed, apparently sixfold symmetric LEED pattern. The crystallinity of the Ag film should be very good in regard to the low R factors of 0.21. Homoepitaxial growth of Ag on a bulk terminated Ag(111) surface shows clustering as high as 20 ML (Ref. 27) at RT with a similar deposition rate of Ag to that of the current experiment. Thus, the growth of flat, 9 ML thick Ag film on an Al(111) surface is quite an unexpected observation.

Our observation of the initial loss of LRO and its nearly perfect recovery agrees with previous results.[17–19] But there is still no comprehensive, microscopic model explaining the abrupt disappearance and gradual recovery of LRO with Ag deposition on an Al(111) surface. Frick *et al.*[17,18] suggested that the formation of Ag islands with a substantially contracted lattice caused the initial loss of LRO. They ignored the possible influence of alloy formation near the interface on the LRO.

In a study of Al on Ag(111) and Ag(110) surfaces, Wytenberg Ormered, and Lambert[16] could assign an AES peak with its transition energy, 61 eV, as originating from the $I_{2,3}N_{4,5}N_{4,5}$ Auger transition of Al from Ag_2Al alloy rather than from the $L_{2,3}VV$ transition of Al atoms. They also found that the AES peak (61 eV) increased in the early stage of Al film growth and decrease with further Al deposition. The Ag/Al(111) system is made in the opposite order of Al/Ag(111). Figure 4(a) shows, however, a similar trend of the intensity variation of the Auger peak. Figure 4(b) shows the variation of each peak intensity estimated from peak-to-peak heights in differential spectra, as a function of Ag coverage. The alloy peak with 61 eV transition energy shows substantial intensity only for those Ag coverages where the LEED pattern disappears. A decreasing peak with its transition energy of 66 eV is from Al atoms ($L_{2,3}VV$ transition) and a growing peak with 46 eV is from pure Ag atoms. This indicates that some of the Ag atoms also from an Ag_2Al alloy with the Al atoms from the substrate, and the surface alloying appears to be correlated with the disappearance of LRO with the deposition of Ag on the Al(111) surface.

Additional evidence for interface alloying comes from x-ray photoelectron spectroscopy XPS data. In Fig. 5(a), Ag($3d_{5/2}$) core-level XPS spectra for Ag films deposited on Al(111) at RT with thicknesses up to 3.8 ML are shown. All

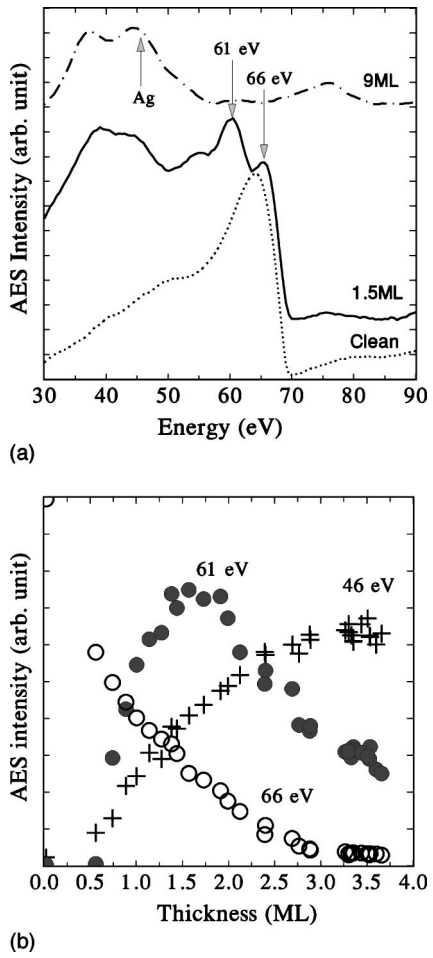

FIG. 4. AES intensity versus Ag thickness. (a) AES spectra for clean Al(111), Ag (1.5 ML)/Al(111), and Ag (9 ML)/Al(111). (b) AES intensity for various Ag thickness. The Auger electron transition energies are 66 eV (open circle), 61 eV (filled circle), and 46 eV(+).

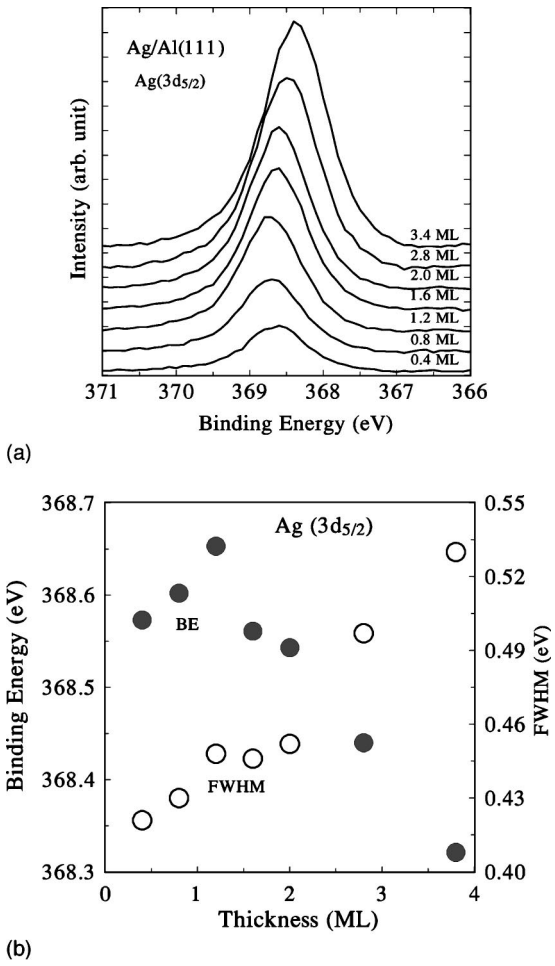

FIG. 5. (a) XPS spectra of Ag ($3d_{5/2}$) as a function of Ag film thickness. (b) The binding energy (closed circle) and FWHM (open circle) versus Ag film thickness.

peak positions of the Ag($3d_{5/2}$) spectra are higher in binding energy (BE) than the well known BE of the bulk Ag($3d_{5/2}$), 368.2 eV.[28] The highest BE shift occurs at 1.2 ML of the Ag film, and the BE is 368.7 eV [Fig. 5(b)]. Fuggle *et al.*[29] reported that the BE of Ag($3d_{5/2}$) from Ag_2Al bulk alloy is higher by 0.5 eV than that of the bulk Ag, and so we may attribute the observed high BE shift of Ag($3d_{5/2}$) for the Ag films to Ag_2Al alloy formation. As the Ag film gets thicker, the center of the peak shifts back toward the lower binding energy side, i.e., toward the bulk Ag peak, and the spectra gets broader. This is caused by the increased contribution from the pure Ag atoms as the film gets thicker.

Another notable feature of the spectra in Fig. 5(a) is the increase of peak width according to the increase of the thickness of Ag film. The Lorentzian widths of Ag $3d_{5/2}$ peaks in Fig. 5(a), which are obtained from a fitting procedure with Voigt function and with a Gaussian width of 0.9 eV (instrumental resolution), are plotted in Fig. 5(b). As one can see from the figure, the full width at half maximum (FWHM) of Ag $3d_{5/2}$ at 3.8 ML thick Ag film is 0.53 eV, which is larger nearly by two times than the value of the pure bulk Ag 0.281 eV.[28] This large broadening of the Ag $3d_{5/2}$ peak implies that there exist more than two peaks in the spectra, originating from Ag atoms with different chemical environment: (1) Ag alloyed with the Al substrate and (2) Ag in pure Ag clusters. Hence, the main features observed in Ag $3d_{5/2}$ core level XPS spectra can be explained consistently under the assumption of interface alloying between deposited Ag atoms and the Al substrate.

Figure 6 shows the results of an oxygen titration experiment. The filled circles indicate the ratio of Auger intensities of oxygen (506 eV) with respect to Ag (357 eV). The ratio decreases rapidly as the Ag coverage increases. The reactivity of Ag at the given titration condition is negligible. Thus, it suggests that the Al exposed to the surface diminishes with Ag coverage, and the alloy formation of Ag and Al is restricted to the interface region of thickness of two to three ML's as also suggested from the above spectroscopic studies.

From the above results of AES, XPS, and oxygen titration at room temperature, we expect that an Ag_2Al alloy forms near the interface and there could be some correlation between the alloy formation near the interface and the loss of LRO. This expectation is strengthened by the behavior of the

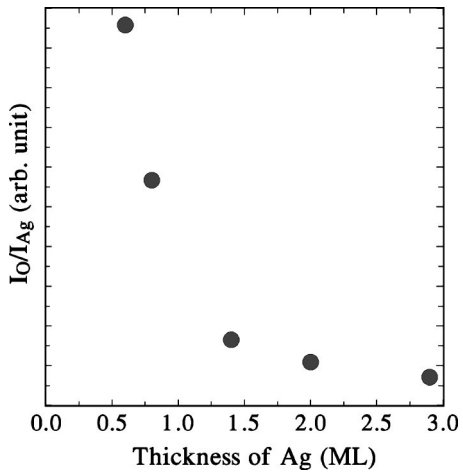

FIG. 6. Oxygen titration results. The amount of oxygen adsorbed on the surface is calibrated by AES intensity of O (transition energy: 506 eV) relative to that of Ag.

Ag film deposited on the Al(111) surface at 50 K. We examined the LEED pattern and Auger spectra at the same low temperature after depositing Ag. On visual inspection, the LEED spot intensity showed the same propensity: a rapid decrease of spot intensities up to 4 ML and a gradual recovery with further Ag deposition, as in Fig. 1(b). However, the LEED patterns were never extinguished, although the spots became very dim and broad in the large background intensity. In Fig. 7, the AES spectra taken for the Ag films deposited on the Al substrate at 50 K still reveal the peak from the alloy, although reduced in intensity, as a small peak or a shoulder near 61 eV. Instead, the intensity of pure Ag (46 eV) relative to that of the Ag_2Al alloy (61 eV) is larger for the film deposited on a substrate at 50 K than that for the film of the same thickness, but deposited on a substrate at RT. This should result from a kinetically limited alloy formation in such a low temperature due to the reduced interdiffusion of Al and Ag. In summary, we find a less severe loss of LRO with reduced interface alloying, which strengthens our suggestion that there is a correlation between the surface alloying and the loss of LRO.

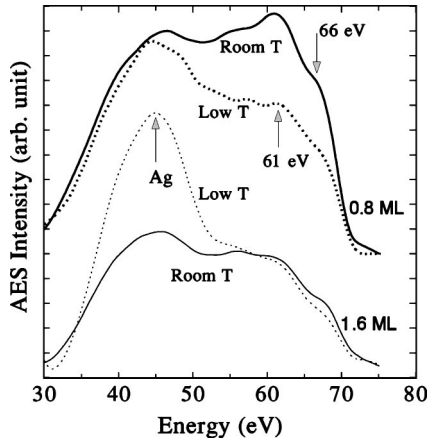

FIG. 7. AES spectra for 0.8 and 1.6 ML Ag deposited on Al(111). Growth temperatures are room temperature (solid line) and 50 K (dotted line).

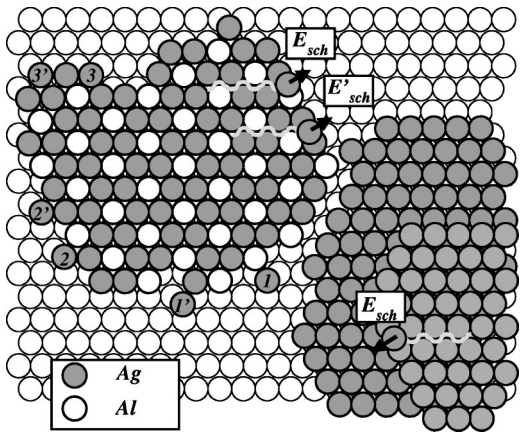

FIG. 8. Adsorption energy per Ag adatom was calculated for both alloy position (marked with unprimed coordination number) and nonalloy position (marked with primed number) at the edge of a Ag_2Al island. Diffusion barrier for a Ag adatom was calculated following the minimum energy path (gray line) from a certain position in the upper terrace near the step edge to the lower terrace with fully relaxed geometry by total energy minimization. Two different cases for interlayer diffusion on Ag_2Al are marked as E_{sch} and E'_{sch}, where the former runs down to the alloy position and the latter to the nonalloy position. Interlayer diffusion of a Ag adatom on an Ag island on an Ag covered surface, as is shown in right corner of the figure was also calculated.

In order to get a microscopic picture on the growth of Ag on an Al(111), we employed a method of semiempirical calculation, embedded-atom method (EAM) by Daw and Baskes.[30] By incorporating a bond bending term, a modified EAM (MEAM) (Ref. 31) has widened applicability even to surface problems of large systems.[32] We used a MEAM code from Baskes,[31] and chose input parameters reproducing well-known diffusion barriers for the homoepitaxial growth of Al and Ag. Details of our MEAM work will be described elsewhere.[33] A reliable quantitative description of elementary kinetic processes requires highly accurate knowledge of the electronic structure of the system of concern. In principle, first-principles calculation should be preferred for such a purpose, but, in practice, are severely limited by computing power for large systems. MEAM calculation with its intrinsic limitations still proved effective to elucidate an atomistic growth process at a qualitative level.[34]

Current MEAM calculations show that the Ag adatom favors the site that forms the Ag_2Al alloy (alloy site) with a difference of the adsorption energies between the alloy site and the nonalloy sites of 0.1–0.2 eV, depending on the nearest-neighbor number (see Fig. 8 and its figure caption). Further, the Erlich-Schwöbel barrier for an Ag atom on an Ag_2Al(island)/Al(111) downward to the alloy formation site (E_{sch}) is dramatically lower than those (E'_{sch}) to the nonalloy sites on the terrace. The respective diffusion path is shown in Fig. 8, and the respective adsorption energies are given in Fig. 9(a). The above results support that the alloy site is energetically preferred for incoming Ag atoms and that the formation of the alloy effectively reduces the interlayer diffusion barrier and helps to extend Ag_2Al islands.

Nevertheless, there is still a missing link that microscopi-

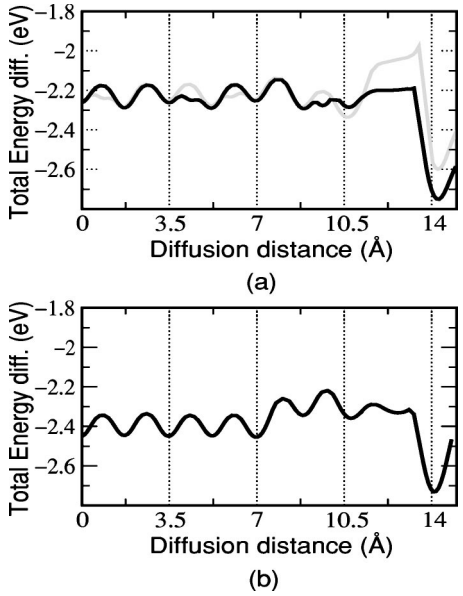

FIG. 9. Adsorption energy per a Ag adatom along each diffusion path as explained in Fig. 8. (a) black (gray) line: Starts from upper terrace of Ag_2Al island down to the alloy (nonalloy) position on Al(111) substrate. (b) interlayer diffusion from a position on a Ag island down to a Ag surface on an Al substrate. Diffusion path is optimized with total energy minimization. Each vertical grid corresponds to the unit diffusion distance, from fcc to fcc via hcp site and vice versa.

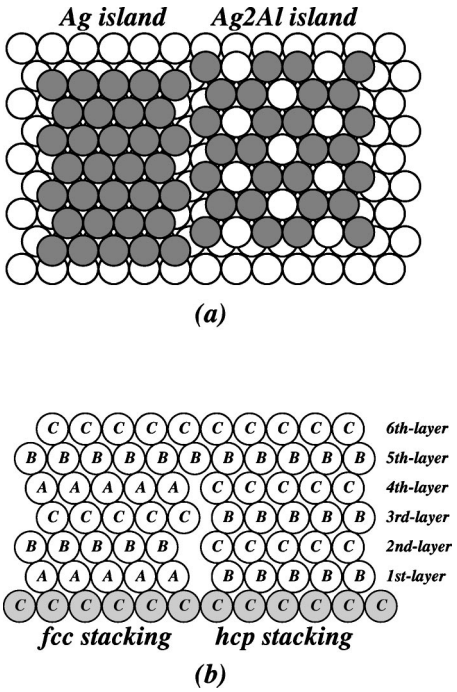

FIG. 10. (a) A schematic top view of possible Ag_2Al and Ag domain arrangement on fcc(111) surface. Filled circles denote Ag atoms and open circles are Al atoms. Ag_2Al island (right) sit on hcp site and Ag cluster (left) sit on fcc site, and dislocation exists between two types of domains. (b) Side view of two types of stacking. fcc stacking (left; $A/B/C$), hcp stacking (right; B/C).

cally connects the interface alloy formation to the loss of LRO in the growing film. In the following section, we propose a qualitative model to explain the microscopic origin of the loss of LRO and possibly the recovery of LRO.

IV. DISCUSSION

The lattice parameter of the Ag_2Al alloy is 2.885 Å,[14] which is almost the same as Ag(2.889 Å) and Al(2.863 Å), so that the structural disorder is not caused by lattice mismatch. It is known, however, that Ag_2Al forms in the hcp structure.[11] So, the stacking faulted hcp islands grow on the fcc Al substrate. Thus, when Ag atoms are deposited on Al(111), some of them form hcpAg_2Al islands and the others fcc Ag islands. Then, they are separated by stacking faulted regions. (Ag atoms on Al(111) favor fcc sites with the adsorption energy larger only by 0.02 eV per atom than that on hcp sites according to our MEAM calculation. Then, hcp pure Ag islands would also nucleate randomly at RT. They are, however, expected to quickly switch to fcc stacking as they grow, as for the case of Al homoepitaxial growth on a (111) surface.[34,35] Hence, we do not take their temporal existence into our account.)

With further deposition, Ag_2Al alloy formation should be reduced. Ag atoms are, however, known to grow on Ag_2Al in hcp stacking up to 6 ML.[19] Hence, the stacking faulted islands would grow as separated before some critical coverage is reached where LRO starts to recover. Since the lateral size of the randomly nucleated islands is limited by the stacking faulted boundaries, they would suffer from severe lattice relaxation to compensate the reduced coordination of the atoms at the edges of the islands as found in spot profile analysis LEED experiments.[18] Those differently stacked, severely relaxed islands and the large density of misfit boundaries between them produce lateral disorder. Further, the intermixing of Ag and Al atoms in the alloy islands propagates the compositional disorder into the substrate as evidenced by the severe reduction in (0,0) intensity in its out-of-phase condition [Fig. 2(b)]. Recently, Wetli, Hochstrasser, and Erbudak[19] reported that Ag films on Ag_2Al grew in hcp structure up to 2–6 ML, and hcp and fcc structures coexisted in the 6–40 ML range without displaying any LEED pattern. That result supports our argument that attributes the loss of LRO to the coexistence of small hcp and fcc islands.

Continued Ag deposition will make the fcc Ag islands and hcp islands grow up, but for the fifth and sixth layers, the adsorption sites of Ag both on fcc islands and on hcp islands are identical as shown in Fig. 10. (Let *ABC* be the stacking sequence of substrate Al, and *C* be the stacking of the surface layer. On top of it, fcc stacking goes *ABCABC* and hcp stacking, *BCBCBC*. We find the fifth and sixth stacking are identical, i.e., *B* and *C*.) Hence, in the fifth and sixth layers, there are no stacking faulted sites and extended islands can form. On top of those layers, fcc stacking, which is natural for bulk Ag, would be preferred. This picture is consistent with our experimental observation, i.e., the recovery of LEED patterns starts from the fifth layer (Fig. 1). On the completion of the sixth layer, however, the recovery of LRO is still not complete, as judged by the low LEED intensity in Fig. 2.

This means that there should still be a large density of unfilled stacking faulted boundary sites and twin boundary sites, as revealed in our LEED I/V analysis. The correction of such misfit sites takes place through many layers on top of the fifth layer due to some kinetic or energetic limitations.

For 9 ML thick film, our LEED I/V analysis, as mentioned in the former section, was successfully made by a model with a flat fcc Ag surface. This implies that large terraces of fcc stacking form with sizes comparable to the coherence length of the incident electrons. This self-correcting growth behavior of Ag from the fifth layer is in sharp contrast to the homoepitaxial growth of Ag film on an Ag(111) substrate that produces high rising clusters (up to 20 ML) at room temperature.[27] The observation of wide terraces of the Ag film ($>$ 5 ML) on Al(111) implies that the interlayer diffusion barrier, the Erlich-Schwöbel barrier, for Ag/Ag ($>$5 ML)/Al(111) should be much smaller than that for Ag/Ag(111), 0.12 eV. Our MEAM calculation on the interlayer diffusion barrier, however, does not satisfy this condition. For a Ag atom on an Ag island/Ag($1M$)/Al(111), the Erlich-Schwoebel barrier is still high, 0.12 eV. [Fig. 9(b)], which is virtually identical to the barrier felt by a Ag atom on Ag(111). Thus, the observed layer-by-layer growth comes from other causes.

A possible clue is that the templates for the homoepitaxial growth of Ag from the fifth layer on, are not as perfect as the clean Ag(111) substrate. Rather, they should still contain a large density of voids and kinks originating from the boundaries of stacking faulted islands. Even for the 9 ML thick film, there should be a large density of kink sites associated with boundaries of twin domains, as revealed by our LEED I/V analysis. For the homoepitaxial growth of Pt on (111) surface, the reentrant, layer-by-layer growth was reported and attributed to the large densities of kink sites formed in the earlier cluster growth.[36] Those kinks offered kinetic paths to promote interlayer diffusion. We expect that the large density of kink sites in the Ag templates would play the same role offering efficient channels for the interlayer diffusion and result in a layer-by-layer growth as for the case of reentrant Pt homoepitaxy on (111) surface. To clarify this descriptive model, studies employing local probes such as scanning tunneling microscope are highly required.

V. SUMMARY AND CONCLUSION

The initial growth mode of ultrathin Ag films on an Al(111) surface was studied. As silver is deposited on an Al(111) at room temperature, intensities of LEED spots diminished exponentially up to about 2 ML, and the LEED pattern completely disappeared from 2 to 4 ML coverage. With further deposition of Ag, (1×1) LEED spots start to reappear. AES, XPS, and oxygen titration experiment showed that a substantial amount of alloying happens near the interface, though the influence of the interface alloying on the growth mode of Ag films has not been taken seriously before.

From our experimental observation, a growth model of Ag on an Al(111) surface is proposed; in the interface, alloying results in Ag_2Al domains of hcp stacking in parts of the surface and on the remaining surface Ag islands of fcc stacking form. On top of those islands, Ag grows following the same stacking of the island where Ag landed. These stacking faulted random islands with large lateral contraction result in the loss of long-range order. For the fifth and sixth layers, however, hcp and fcc stacking find the same adsorption sites, resulting in more natural fcc stacking of Ag from the fifth layer on. Ag films ($>$5 ML) display large terraces as evidenced by sharp LEED spots, which is at variance with the growth mode of Ag on a clean Ag(111) surface. A large density of kink sites originating from the stacking faulted domain boundaries are expected to offer efficient interlayer diffusion channels. This kind of growth mode is similar to the reentrant growth of Pt on (111) surface.

ACKNOWLEDGMENTS

We thank M. Baskes, K. Takahashi, M. Scheffler, J. Wollschläger, and W. Wulfhekel for helpful comments. J.K. thanks S. Cho for the technical support and C. Ihm for the low-temperature experiment. This work was supported in part by KOSEF through ASSRC and by Nanotechnology Project ('99) from MOST, by Korea Research Foundation (1998-015-D00119), and by the ministry of science and technology (99-N6-02-01).

*Present address: Fritz-Haber Institut der Max-Planck Geselschaft.

[1] H. Brune, Surf. Sci. Rep. **31**, 121 (1998), and references therein.

[2] Z. Zhang and M. G. Lagally, Science **276**, 377 (1997); *Morphological Organization in Epitaxial Growth and Removal*, edited by Z. Zhang and M. G. Lagally (World Scientific, Singapore, 1998).

[3] H. Brune and K. Kern, in *The Chemical Physics of Solid Surface*, edited by D. A. King and D. P. Woodruff (Elservier Science, Amsterdam, 1997), Vol. 8, p. 149; H. Ibach, Surf. Sci. Rep. **29**, 193 (1997).

[4] J. C. Hamilton, R. Stumpf, K. Bromann, M. Giovannini, K. Kern, and H. Brune, Phys. Rev. Lett. **82**, 4488 (1999); C. Ratsch, A. P. Seitsonen, and M. Scheffler, Phys. Rev. B **55**, 6750 (1997).

[5] F. Besenbacher, L. P. Nielsen, and P. T. Sprunger, in *The Chemical Physics of Solid Surface*, edited by D. A. King and D. P. Woodruff (Elsevier Science, Amsterdam, 1997), Vol. 8, p. 207.

[6] U. Bardi, Rep. Prog. Phys. **57**, 939 (1994).

[7] S.-K. Kim, J.-S. Kim, J. Han, J. M. Seo, C. K. Lee, and S. C. Hong, Surf. Sci. **453**, 47 (2000).

[8] C. Stampfl, M. Scheffler, H. Over, J. Burchhardt, M. Nielsen, D. L. Adams, and W. Moritz, Phys. Rev. B **49**, 4959 (1994).

[9] L. Vitos, A. V. Ruban, H. L. Skriver, and J. Kollar, Surf. Sci. **411**, 186 (1998); H. L. Skriver and N. M. Rosengaard, Phys. Rev. B **46**, 7157 (1992).

[10] J. Cai and Y. Y. Ye, Phys. Rev. B **54**, 8398 (1996).

[11] T. M. Massalski, *Binary Alloy Phase Diagrams* (ASM International, New York, 1990).

[12] B. Fischer, J. V. Barth, A. Fricke, L. Nedelmann, and K. Kern, Surf. Sci. **389**, 366 (1997); B. Fischer, H. Brune, J. V. Barth, A. Fricke, and K. Kern, Phys. Rev. Lett. **82**, 1732 (1999).

[13] K. Wilson, J. Brake, A. F. Lee, and R. M. Lambert, Surf. Sci. **387**, 257 (1997).
[14] V. Shutthanandan, Adli A. Saleh, N. R. Shivaparan, and R. J. Smith, Surf. Sci. **350**, 11 (1996).
[15] N. R. Shivaparan, V. Shutthanandan, V. Krasemann, and R. J. Smith, Surf. Sci. **365**, 78 (1996); G. W. Anderson and P. R. Norton, *ibid.* **336**, 262 (1995); A. M. Begley, D. Tian, F. Jona, and P. M. Marcus, *ibid.* **280**, 289 (1993).
[16] W. J. Wytenburg, R. M. Ormerod, and R. M. Lambert, Surf. Sci. **282**, 205 (1993).
[17] B. Frick and K. Jacobi, Surf. Sci. **178**, 907 (1986).
[18] B. Frick, K. Jacobi, G. Meyer, and M. Henzler, Solid State Commun. **63**, 475 (1987).
[19] E. Wetli, M. Hochstrasser, and M. Erbudak, Surf. Sci. **377–379**, 876 (1997); M. Erbudak, M. Hochstrasser, and E. Wetli, J. Electron Spectrosc. Relat. Phenom. **76**, 529 (1995); E. Wetli, M. Erbudak, and D. D. Vvedensky, Surf. Sci. **317**, 235 (1994).
[20] A. Losch and H. Niehus, Surf. Sci. **446**, 153 (2000).
[21] W. Kim, W. Kim, S.-J. Oh, J. Seo, J.-S. Kim, H.-G. Min, and S.-C. Hong, Phys. Rev. B **57**, 8823 (1998); S. H. Kim, K. S. Lee, H. G. Min, J. Seo, S. C. Hong, T. H. Rho, and J.-S. Kim, *ibid.* **55**, 7904 (1997); K. S. Lee, S. H. Kim, H. G. Min, J. Seo, and J.-S. Kim, Surf. Sci. **377–379**, 918 (1997).
[22] M. A. van Hove and S. Y. Tong, *Surface Crystallography by LEED* (Springer-Verlag, New York, 1979); P. J. Rous, Prog. Surf. Sci. **39**, 3 (1992).
[23] V. L. Moruzzi, J. F. Janak, and A. R. Williams, *Calculated Electronic Properties of Metals* (Pegarmon, New York, 1978).
[24] W. F. Egelhoff, J. Vac. Sci. Technol. **20**, 668 (1982).
[25] R. J. Smith (private communication).
[26] M. Henzler, Surf. Sci. **357–358**, 809 (1996).
[27] J. Vrijmoeth, H. A. van der Vegt, J. A. Meyer, E. Vlieg, and R. J. Behm, Phys. Rev. Lett. **72**, 3843 (1994).
[28] P. H. Citrin, G. K. Wertheim, and Y. Baer, Phys. Rev. B **27**, 3160 (1983).
[29] J. C. Fuggle, E. Kallne, L. M. Watson, and D. J. Fabian, Phys. Rev. B **16**, 750 (1977).
[30] M. S. Daw, M. I. Baskes, Phys. Rev. Lett. **50**, 1285 (1983); M. S. Daw and M. I. Baskes, Phys. Rev. B **29**, 6443 (1984).
[31] M. I. Baskes, Phys. Rev. B **46**, 2727 (1992).
[32] M. I. Baskes, Modell. Simul. Mater. Sci. Eng. **5**, 149 (1997); K. Takahashi, C. Nara, T. Yamagishi, and T. Onzawa, Appl. Surf. Sci. **151**, 299 (1999).
[33] Y. H. Shin, J. K. Seo, and J.-S. Kim (unpublished).
[34] J. C. Hamilton, M. S. Daw, and S. M. Foiles, Phys. Rev. Lett. **74**, 2760 (1995).
[35] R. Stumpf and M. Scheffler, Phys. Rev. B **53**, 4958 (1996).
[36] J. Jacobsen, K. W. Jacobsen, P. Stoltze, and J. K. Norskov, Phys. Rev. Lett. **74**, 2295 (1995).